Journal of Colloid and Interface Science 337 (2009) 81–87

Contents lists available at ScienceDirect

Journal of Colloid and Interface Science

www.elsevier.com/locate/jcis

Effect of PEG on rheology and stability of nanocrystalline titania hydrosols

Pierre Alphonse *, Rudina Bleta, Regis Soules

Université de Toulouse, CIRIMAT UPS-CNRS, 118 route de Narbonne, 31062 Toulouse cedex 9, France

ARTICLE INFO

Article history:
Received 10 March 2009
Accepted 25 April 2009
Available online 12 May 2009

Keywords:
Sol–gel
Titanium dioxide
Colloid
Nanofluid
Rheology
PEG

ABSTRACT

Very stable titania hydrosols were prepared by fast hydrolysis of titanium isopropoxide in a large excess of water. XRD patterns show that these sols contain nanocrystals (5–6 nm) of anatase (70%) and brookite (30%). TEM images indicate that these primary particles form aggregates whose mean hydrodynamic diameter, determined by photon correlation spectroscopy, is in the range of 80–90 nm. The flow curves of these colloids, recorded for several volume fractions of nanoparticles, can be perfectly fitted, in the range 0–100 s^{-1}, with a power-law model. In this range the behavior is Newtonian but for larger shear rates a shear thinning is observed. The viscosity dependence on particle concentration can be predicted by a Batchelor-type model were the volume fraction of particles is replaced by an effective volume fraction of aggregates, taking into account their fractal dimension. Addition of polyethylene glycol (PEG 2000) induced a marked decrease (more than 50%) of the sol viscosity down to a minimum. This is explained by assuming that PEG adsorbs on the surface of TiO_2 particles producing stabilization by steric effects and leading to formation of more compact aggregates. Without PEG the sol viscosity strongly decreases on aging. This effect is not caused by the growth of primary particles. It is rather interpreted as a progressive reorganization of the aggregates toward a more compact packing.

1. Introduction

Titanium dioxide coatings, with large specific surface areas and controlled porosity, have wide applications in different fields such as solar energy conversion [1], photocatalysis [2], and catalysis [3,4]. Among the different synthesis routes used to produce titania films, the sol–gel method is ubiquitous because it has many advantages such as purity, homogeneity, control over the microstructure, ease of processing, low cost, and the ability to coat large and complex substrates.

By mastering size and organization of the nanoparticles in colloidal suspensions, titania films with controlled porosity and surface area can be synthesized. These nanoparticles are usually prepared from the hydrolysis and condensation of titanium alkoxides in water. In presence of a large excess of water ($w = [H_2O]/[Ti] \approx 100$), hydrolysis is very fast and nucleation and particle growth are completed within a few seconds, producing ultrafine primary particles whose size ranges from 2 to 8 nm [5]. These nanoparticles agglomerate very rapidly, producing large precipitates of macroscopic dimensions [6]. It was shown that, upon aging, such precipitates give a mixture of anatase and brookite [7]. Peptization through the action of an inorganic acid (HCl or HNO_3) is often used to break up the aggregates. The final result is a translucent suspension containing particles whose size ranges from 15 to 100 nm. Since the final size is still larger than the size of the primary particles, these peptized colloids consist of agglomerated structures containing several primary particles [6]. Peptization is a slow process that exhibits first-order kinetics [8] with time constants of several days [6]. But peptization time can be reduced by increasing either the temperature (>80 °C) or the acid concentration [7]. The effects of parameters like the pH, the hydrolysis and peptization temperature, and the alkoxide alkyl group have been studied. It was found that the size of titania nanoparticles is mainly controlled by colloidal interactions, whereas chemical factors, such as the rate of hydrolysis and condensation, have a secondary role [9].

Though the synthesis of titania films by the sol–gel process has been extensively studied, most of the sols used in the reported procedures have shown a very limited stability (<24 h). It should be emphasized that, for a large scale production of titania coatings (for example, by roll-coating), a long term stability of the titania sol is needed in order to achieve an acceptable repeatability. Nevertheless the peptized sols are prone to reagglomeration and the increase of size can lead to flocculation. The poor stabilization of nanosized titania has led to the hypothesis that the slow peptization is the result of the simultaneous action of two opposing mechanisms: (i) the fragmentation of primary particle agglomerates by the peptizing agent, and (ii) the coarsening, which is driven by the solid concentration, the titania solubility (which depends on pH),

* Corresponding author. Fax: +33 561 556 163.
E-mail addresses: alphonse@chimie.ups-tlse.fr (P. Alphonse), bleta@chimie.ups-tlse.fr (R. Bleta), regis.soules@pca.ups-tlse.fr (R. Soules).
URL: http://www.cirimat.cnrs.fr/ (P. Alphonse).

0021-9797/$ - see front matter © 2009 Elsevier Inc. All rights reserved.
doi:10.1016/j.jcis.2009.04.087

and the size polydispersity [6,10]. Coarsening involves the growth of larger particles at the expense of smaller ones (Ostwald ripening).

Catalytic applications require a tunable porosity to optimize the diffusion rate of reactants toward the adsorption sites and a high surface area to maximize the interface between the reactant flow and the catalyst surface. To control the porosity of titania xerogels, polymers or structure directing agents are added to the sols before or after the peptization [11–18]. These additives are removed by calcination of the xerogels in air. However because these additives interact with titania particles, they could have a strong effect on the stability and rheology of the sols. Therefore knowledge of this influence is mandatory in order to achieve the synthesis of reproducible catalytic films with controlled thickness and porosity.

In this paper the effect of polyethylene glycol (PEG) on the stability and rheology of titania sols is investigated. PEG is a widely used additive, but most of the studies were focused on the characterization of the microstructure of xerogels and very few are considering its influence on the properties of the colloidal suspensions.

2. Experimental

2.1. Sol synthesis

Titania sols were prepared by hydrolysis of titanium alkoxide in a large excess of water. This method gives colloids of titania nanocrystallites dispersed in water [14,5]. The following procedure was optimized to give crystallites as small as possible and to produce stable sols. Hot (80 °C) distilled water (H_2O/Ti ≈ 90) was added quickly, under vigorous stirring, on titanium (IV) isopropoxide dissolved in isopropyl alcohol (C_3H_8O/Ti = 3.5). A white precipitate was obtained. After 5 min, a solution of nitric acid (H^+/Ti = 0.2) was added to the suspension and the mixture was kept under stirring for 16 h at 80 °C. The white suspension changed gradually to a translucent sol by peptization. At the end of peptization the pH of the sol is close to 1.0. More concentrated sols were obtained by evaporation at 80 °C until the required concentration was reached. A slight increase in pH was observed after concentration, i.e., pH ≈ 0.5 for a titania concentration of 10 wt%.

2.2. Rheology

Rheology mesurements on the sols were done with a rheometer Anton Paar Physica MCR fitted with a cone and plate device. The dimensions corresponding to the geometry were 50 mm for the diameter and 1° for the angle. The minimum distance between plate and truncated cone was 0.05 mm. Rheograms were recorded at 20 °C, with shear rate being stepwise increased and decreased over the range of 1–1000 s^{-1}, with a total time period of 300 s for both the increasing and the decreasing shear rate sweeps. For each sample, a minimum of four measurements was performed. For the lowest shear rates (typically below 10 s^{-1} some fluctuations of viscosity were observed, especially in the case of the less viscous sols.

2.3. Zeta potential and particle hydrodynamic diameter

Electrophoretic mobility and particle hydrodynamic diameters were determined on a Malvern Zetasizer 3000 using a He–Ne laser as light source (λ = 633 nm). The zeta potential was calculated from electrophoretic mobility using the Henry equation and Smoluchowski approximation

Particle sizes were measured by photon correlation spectroscopy (PCS). All size measurements were done at 25 °C with a scattering angle of 90°. To control the effect of multiple scattering and particle interactions, analysis were performed at several dilutions in order to check that the measured size was not dependent on the dilution.

2.4. Powder X-ray diffraction (PXRD)

The crystal structure was investigated by powder X-ray diffraction. Data were collected, at room temperature, on a Bruker AXS D4 θ–2θ diffractometer, in Bragg–Brentano geometry, using filtered CuKα radiation and a graphite secondary-beam monochromator. Diffraction intensities were measured by scanning from 20° to 80° (2θ) with a step size of 0.02° (2θ). Crystalline structures were refined using FullProf software [19]. The peak profiles were modeled by pseudo-Voigt functions. The refined FWHM (full-width at half-maximum) of the lines was used to compute, by the Scherrer equation, the average crystallite size [20]. The instrumental broadening contribution was evaluated by using a highly crystalline rutile sample as standard.

2.5. Specific surface area and density

The specific surface areas were computed from the adsorption isotherms, using the Brunauer–Emmett–Teller (BET) method [21]. Adsorbate was nitrogen and isotherms were recorded at 77 K with a Micromeritics ASAP 2010M.

Skeletal densities of powders were determined using a gas pycnometer (Micromeritics AccuPyc 1330) working with helium. Each experimental value results from the average of 10 successive measurements on the same sample.

2.6. Electron microscopy

High resolution transmission electron microscopy analyses were performed on a JEOL 2100F operating at 200 kV. Conventional TEM observations were done on a JEOL 1011 operating at 100 kV. Samples were prepared by dipping a carbon-coated grid in a sol diluted 50 times in water. Then the grid was allowed to dry for 48 h at room temperature.

3. Results and discussion

3.1. Characterization of titania hydrosols

XRD pattern (Fig. 1) shows that titania sols dried at room temperature contain two crystalline phases, anatase (tetragonal, $I4_1/amd$, JCPDS No. 00-021-1272) and brookite (orthorhombic, Pbca,

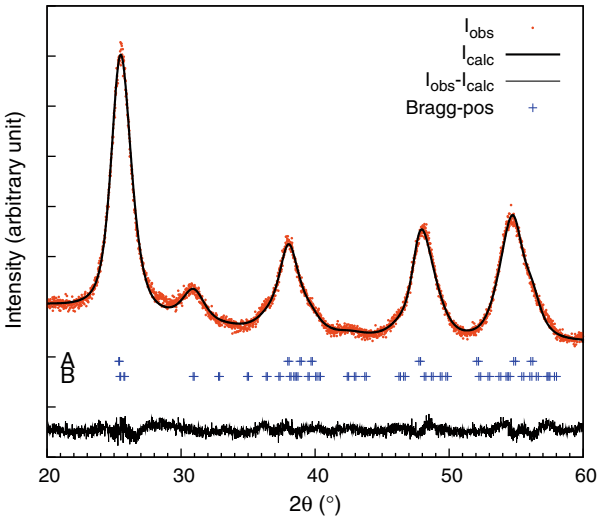

Fig. 1. XRD powder pattern of a titania xerogel dried at 30 °C. Experimental pattern (dots) and whole-pattern decomposition (line) computed for a mixture of anatase (A: tetragonal unit cell, space group No. 141, $I4_1/amd$) and brookite (B: orthorhombic unit cell, space group No. 61, Pbca).

JCPDS No. 01-076-1934). Due to the numerous brookite reflections, and to the strong overlap of the diffraction lines (because phases are nanocrystalline), we failed to find an acceptable solution by the Rietveld method. However, the profile matching method (whole-pattern decomposition) gave the cell parameters and the peak profiles for both phases. From the peak width we found an average size for anatase crystallites of ca. 6 nm while the size of brookite crystals was ca. 5 nm. As already reported [22], to determine the phase proportions of anatase and brookite, refinement of the structure by the Rietveld method was done within a 2θ range restricted to 20–35° (2θ). This range includes the (1 0 1) line of anatase, and (1 2 0), (1 1 1), and (1 2 1) lines of brookite. For the refinement, all parameters except the scale factor were fixed. We found by this method a fraction of brookite in the mixture close to 30%.

TEM images (Fig. 2) confirm that the average particle size is 5–6 nm. A selected area electron diffraction (SAED) pattern shows rings of reflections whose intensities and positions are in good agreement with those observed in the XRD pattern (Fig. 1). The images taken at lower magnification show that primary particles have a strong tendency to form aggregates, with a chainlike structure, containing more than 100 particles (Fig. 2). The packing density of these clusters decreases from center to border. It seems probable that boundary particles could be disconnected from such aggregates at high shear rates.

The specific surface area of a sol dried at room temperature (and outgassed at 50 °C for 24 h) is 240 ± 10 $m^2\ g^{-1}$. The specific surface area S_w (in $m^2\ g^{-1}$) of a material composed of spherical particles all having the same diameter D (in nm) can be calculated by the equation

$$S_w = \frac{6}{\rho D}, \tag{1}$$

where ρ is the density of the particles (in kg m^{-3}). This density is supposed to be close to the density of a xerogel prepared by drying the titania sol at room temperature. This xerogel density was measured with a helium pycnometer and found to be 2700 ± 100 kg m^{-3}. However, the average density of a material containing 70% of anatase crystals (ρ = 3900 kg m^{-3}) and 30% of brookite crystals (ρ = 4120 kg m^{-3}) is 4000 kg m^{-3}. This difference can be interpreted by assuming that the numerous hydroxyl groups on the surface of the particles produce a layer having a lower density than the core.

Taking ρ = 2700 kg m^{-3} and D = 6 nm gives a surface area equal to 370 $m^2\ g^{-1}$. This high value compared to the experimental one indicates that primary particles in the core of aggregates are so closely packed that nitrogen cannot have access to their surface.

Another evidence that primary particles agglomerate to give aggregates whose size is large enough to scatter visible light is the fact that these suspensions are not transparent but translucent (milky). The mean hydrodynamic diameter of aggregates, determined by photon correlation spectroscopy, was in the range of 80–90 nm, in good agreement with electron microscopy images.

The zeta potentials of suspensions were in the range of +25 to +30 mV. This rather low repulsive barrier can explain why the peptization process requires 16 h at 80 °C to give a translucent sol.

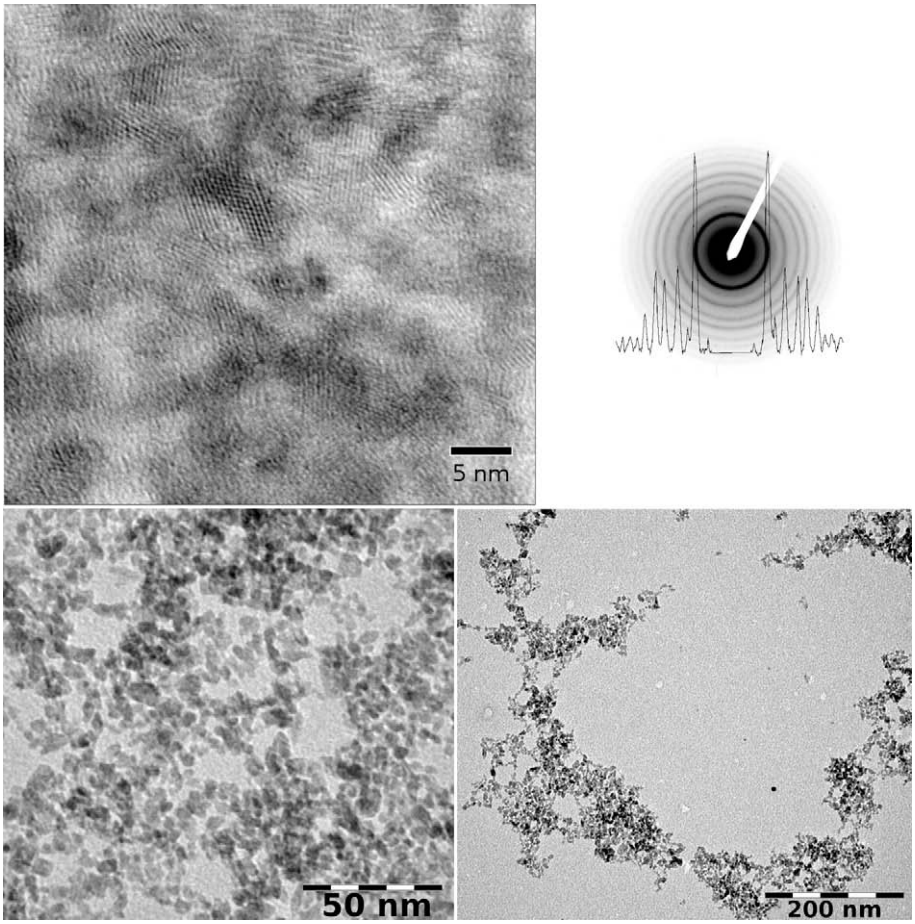

Fig. 2. Upper part: high resolution TEM image and selected area electron diffraction (SAED) pattern. Lower part: medium and low scale TEM images.

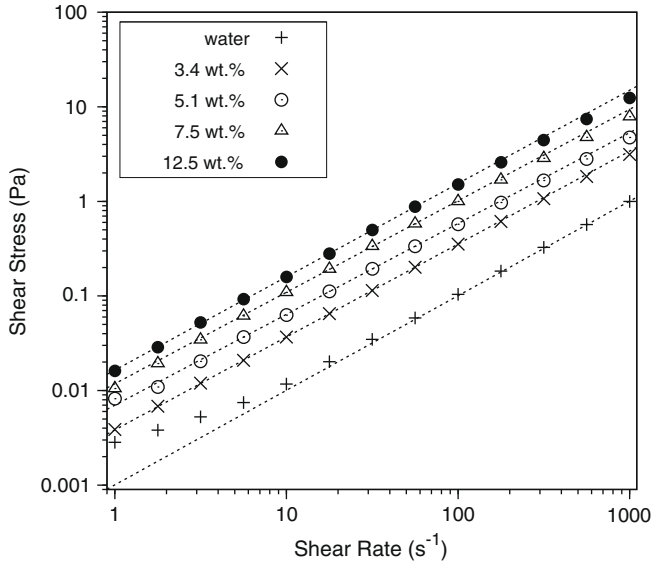

Fig. 3. Effect of titania concentration in sols on shear stress–shear rate curves. Temperature = 20 °C. Lines correspond to the fitting of experimental data points (symbols) by a power-law model (Eq. (3)), in the range 1–100 s^{-1}.

3.2. Effect of TiO_2 concentration (volume fraction)

Concentrations of titania (in g/L) in colloids were calculated from the residual mass after calcination (for 2 h at 800 °C) of a known volume of sol. Assuming volume additivity, the volume fraction of particles, Φ, can be calculated by

$$\Phi = \frac{C}{\rho}, \tag{2}$$

where C is the concentration (in g/L) of TiO_2 in the sol and ρ is the density of titania particles (ρ = 2700 kg m^{-3}).

Rheograms recorded for sols containing increasing amounts of titania are presented in Fig. 3. Rheograms were measured by increasing and then decreasing the shear rate. For each rheogram the curves obtained during reversible shear rate–shear stress paths overlapped; i.e., no hysteresis was observed in any of the studied sols. None of the sols exhibited a Bingham plastic behavior (yield stress can always be approximated to zero). The fitting of the data was done by using the power-law rheological model [23]

$$\sigma = K\dot{\gamma}^n, \tag{3}$$

where σ is the shear stress (Pa), $\dot{\gamma}$ the shear rate (s^{-1}), K the consistency coefficient, and n the power-law index. The results of the least-square fitting of the experimental points are reported in Table 1. In the range 1–100 s^{-1} this model gives an excellent agreement with the experimental data, showing a Newtonian behavior (n very close to 1). For shear rates larger than 100 s^{-1} shear thinning is observed. The behavior observed for water at a low shear rate is probably due to the rheometer geometry used which is inappropriate for low viscosity media.

Table 1
Fitting rheological data, in the range 1–100 s^{-1}, with power-law model, Eq. (3): effect of concentration of titania particles.

Concentration (wt%)	Volume fraction (Φ)	K	Relative error on K (%)	n	Relative error on n (%)
0	0.000	0.001	0.3	1.00	n Fixed
3.4	0.013	0.004	0.3	0.98	0.1
5.1	0.020	0.007	2.0	0.96	0.6
7.5	0.029	0.012	1.6	0.97	0.5
12.5	0.050	0.016	0.8	0.99	0.2

Rheometer temperature = 20 °C.

The viscosity dependence on particle concentration in diluted suspensions is usually expressed as a function of relative viscosity versus volume fraction of the particles [24]. The relative viscosity, η_r, being defined as

$$\eta_r = \eta/\eta_s, \tag{4}$$

where η_s is the viscosity of the dispersion medium (water in our case).

The relative viscosities, measured for several shear rates, are plotted against the volume fraction of nanoparticles in Fig. 4. For low particle volume fractions, as is the case here, the relative viscosity can be predicted by Batchelor's model [25] (valid for $\Phi < 0.1$)

$$\eta_r = 1 + [\eta]\Phi + [\eta]^2\Phi^2, \tag{5}$$

where $[\eta]$ is the intrinsic viscosity defined by

$$[\eta] = \lim_{\Phi\to 0}(\eta_r - 1)/\Phi. \tag{6}$$

For monodisperse dispersions of hard spheres, $[\eta]$ = 5/2 [24].

It was recently shown [26–31] that Batchelor's model strongly underestimates the viscosity measured for nanoscale colloid solutions (so-called nanofluids). This deviation was attributed to particle aggregation. The aggregates can be considered as new particles with an effective diameter D_a. The effective volume fraction Φ_a is given by

$$\Phi_a = \Phi\left(\frac{D_a}{d}\right)^{3-D_f}, \tag{7}$$

where d is the diameter of primary particles and D_f is the fractal dimension of the aggregates. D_f represents the packing change with distance from the center of the aggregate. The lower the value of D_f the more open the packing [23]. The number of particle per aggregate is given by

$$n_a = \left(\frac{D_a}{d}\right)^{D_f}. \tag{8}$$

As in the Eq. (5), relative viscosity will be related to the effective volume fraction Φ_a by

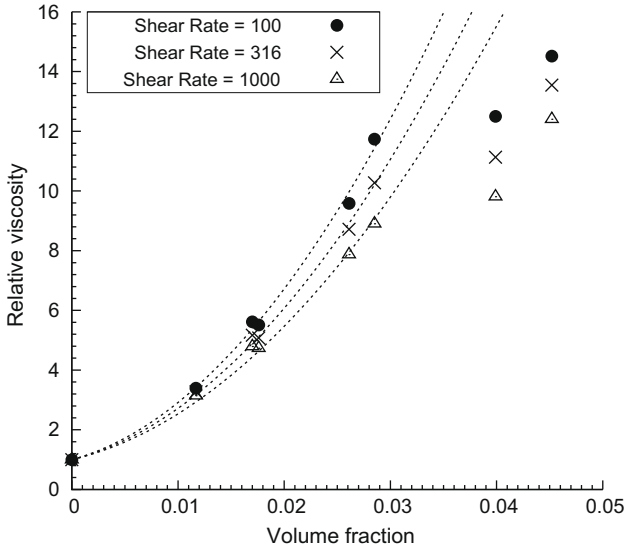

Fig. 4. Relative viscosity dependence on volume fraction of titania particles for several shear rates. Rheometer temperature=20 °C. Symbols correspond to experimental data points. Lines correspond to the best fit of experimental data by Eq. (10) for a titania volume fraction < 0.04.

$$\eta_r = 1 + [\eta]\Phi_a + [\eta]^2\Phi_a^2. \quad (9)$$

Fitting the experimental data $\eta_r = f(\Phi)$ presented in Fig. 4 with the equation

$$\eta_r = 1 + k\Phi + (k\Phi)^2 \quad \text{with } k = [\eta]\left(\frac{D_a}{d}\right)^{3-D_f} \quad (10)$$

gives the best k. Then the ratio D_a/d can be calculated according to the values of $[\eta]$ and D_f. As shown in Fig. 4, a good fit can be obtained if the data for $\Phi > 0.04$ are not taken into account.

Assuming that $[\eta] = 5/2$ (dispersions of hard spheres), to obtain the value of D_a/d we need to know D_f, the fractal dimension of aggregates. In the studies on nanofluids, the authors take $D_f = 1.8$ [27,28,30], which corresponds to diffusion-limited aggregation (sticking probability = 1). In our case, the sols are prepared by peptization, the sticking probability is less than unity, and we are in reaction-limited aggregation regime. In this case $D_f \approx 2.1$–2.2 [32]. However, for titania sols prepared by hydrolysis–peptization of titanium isopropoxide, the values reported for D_f were 1.5 [10] and 1.72 [6]. Moreover, the medium value of zeta potential and the time required for peptization are in favor of a low D_f. The values of D_a/d, calculated for $D_f = 1.8$ and $D_f = 1.7$, are reported in Table 2. At low shear rates and for $D_f = 1.8$, the number of particles in aggregates is 240. This number decreases to 115 if $D_f = 1.7$.

It is noted in Table 2 that the number of particles in aggregates decreases when the shear rate increases. It can be due to a loss, at high shear rate, of loosely bound particles at the boundary of aggregates.

The number of particles in aggregates reported for nanofluids is generally close to 10 [28]. Our larger values can be explained by the fact that our primary particles are smaller and thus have a higher probability of aggregation (as decreasing particle size at constant volume fraction decreases the average interparticle distance, making the attractive van der Waals forces more important [33]). It can be linked with the fact that the relative viscosity of our sols is about three times higher than those reported for larger particles [28].

As shown in Fig. 4 there is a sharp decrease of the relative viscosity for $\Phi > 0.04$. This can be due to some interpenetration of the branch-like parts of aggregates (Fig. 2) leading to a decrease of the effective volume fraction Φ_a.

3.3. Effect of the PEG 2000 addition

Because the nanoparticles have a strong tendency to agglomerate, due to the van der Waals interactions, electrostatic or steric stabilization is usually used to stabilize colloids by creating repulsions between the particles [33]. Electrostatic stabilization consists of the adsorption of ions on the surface of the particles with creation of the electric double layer, whereas steric stabilization can be achieved by the adsorption of large molecules such as polymers forming a dense layer around the particles [34]. Coil dimensions of polymers are usually larger than the range over which attractions between colloidal particles are active [35]. In this study we investigated the effect of post addition of PEG as a surface modifier for the stabilization of titania sols.

Table 2
Fitting relative viscosity with Eq. (10) and assuming $[\eta] = 5/2$ and either $D_f = 1.8$ or $D_f = 1.7$; n_a is calculated by Eq. (8).

Shear rate (s^{-1})	k	Relative error on k (%)	n_a ($D_f = 1.8$)	n_a ($D_f = 1.7$)
10	94	1.12	231	115
100	97	0.93	242	120
316	90	0.71	217	109
1000	84	1.01	193	98

Fig. 5 presents the effect of PEG 2000 addition on the viscosity of sols for several volume fractions of titania particles. Whatever the volume fraction of particles, the addition of low amounts of PEG 2000 induces a large decrease of the sol viscosity. On further PEG addition the viscosity reaches a minimum (about 50–60% of the value observed without PEG) and then it increases steadily. The PEG concentration corresponding to the minimum increased when the volume fraction of titania increased. It can be noted that this minimum is reached for a ratio between the number of ethylene oxide units and the number of titanium atoms (EO/Ti) in the range of 0.3–0.4.

We have observed that addition of PEG 2000 up to 40 g/L (EO/Ti ~ 2) in a diluted sol (titania volume fraction = 0.012) produced a shift toward low diameters of the particle size distribution determined by photon correlation spectroscopy. The mean hydrodynamic diameter of aggregates decreased from 80–90 to about 50 nm.

The decrease of viscosity, resulting from PEG addition, can be interpreted by assuming that PEG adsorbs on the surface of TiO_2 particles producing stabilization by steric effects. This will decrease the sticking probability, which in turn will increase the fractal dimension D_f. As the aggregates become more compact, the effective volume fraction will decrease which finally will decrease the sol viscosity. For example, using Eq. (10), it can be calculated that for $n_a = 120$, increasing the fractal dimension from 1.7 to 1.8 leads to a decrease of relative viscosity of more than 50%.

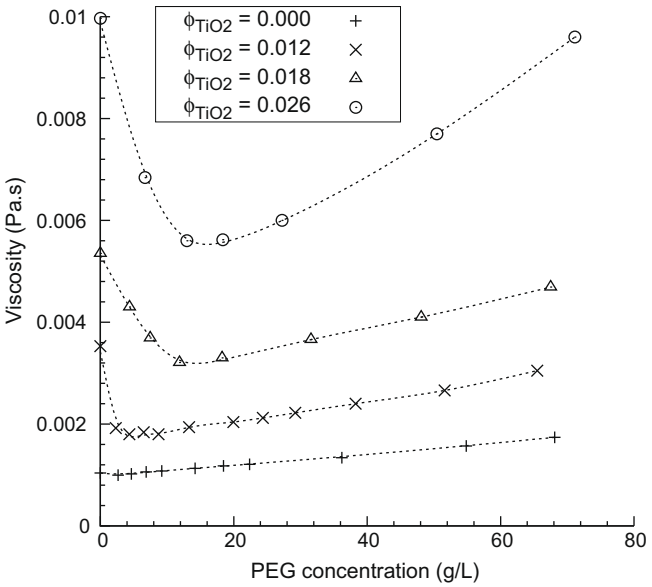

Fig. 5. Effect of addition of PEG 2000 on the viscosity of titania sols. Viscosity was measured at a shear rate of 100 s^{-1}. Rheometer temperature = 20 °C. The dotted lines are shown for visual aid.

Table 3
Fitting rheological data, in the range 1–100 s^{-1}, with power-law model, Eq. (3): Effect of PEG concentration.

PEG 2000 Concentration (g/L)	K	Relative error on K (%)	n	Relative error on n (%)
0	0.011	1.6	0.97	0.5
6.7	0.008	0.3	0.98	0.1
13.0	0.006	1.2	0.99	0.6
18.4	0.007	2.6	0.96	0.4
71.2	0.010	0.7	0.99	0.2

Volume fraction of titania sol, $\Phi = 0.026$. Rheometer temperature=20 °C.

The flow curves were fitted by the power-law rheological model. The results of the least-square fitting for a fixed volume fraction of titania ($\Phi = 0.026$) are reported in Table 3. Again this model gives an excellent agreement with the experimental data. It is noted that the change of viscosity produced by PEG addition is mainly reflected by the consistency coefficient K because the power-law index remains close to unity. Addition of PEG tend to suppress the shear thinning behavior observed for high shear rates. This is in agreement with our previous interpretation because the loss of particles at the external boundary of aggregates at high shear rates will be minimized if aggregates are more compact.

3.4. Effect of aging

To study the effect of aging time on the viscosity, a fresh sol (volume fraction of titania, $\Phi = 0.026$) was prepared and then divided in two parts: one part was kept unchanged while on the other part PEG (18 g/L) was added. The PEG quantity was chosen to be close to the value giving the minimum of viscosity (EO/Ti = 0.4). This second sol was kept under stirring for about 2 h to achieve the complete dissolution of the polymer. A first measurement of the viscosity was performed in both sols (with and without PEG) immediately after the PEG addition starting 2 h after the end of synthesis. Then, the samples were allowed to stand at room temperature. Measurements of viscosity were performed on different time intervals over a period of 45 days (1160 h). It should be emphasized that no sedimentation was observed with these sols even after several months of settling. However, prior to each measurement, the samples were kept under stirring for 10 min in order to ensure the homogenization of the sol.

As shown in Fig. 6, a steady decrease of the viscosity with time was observed even when the sols were not concentrated. After the addition of PEG, the viscosity change was rather low and the sols can be considered stables enough to make reproducible coatings.

Aging produces a broadening of the particle size distribution determined by photon correlation spectroscopy. There is also a slight shift toward large diameters and the mean hydrodynamic diameter increases slightly (≈10 nm).

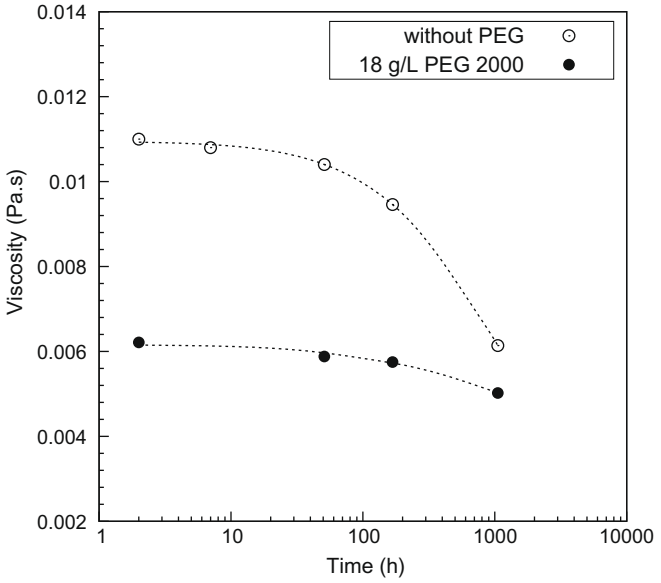

Fig. 6. Effect of aging at room temperature on sol viscosity without and with addition of PEG 2000. Viscosity was measured at a shear rate of 100 s^{-1}. Volume fraction of titania sol, $\Phi = 0.026$. Rheometer temperature = 20 °C. The dotted lines are shown for visual aid.

To check if the effect of aging was not the consequence of Ostwald ripening by dissolution–reprecipitation, we have compared the XRD pattern for a fresh sol with the pattern of an aged sol. Except for a small difference in the first peak intensities, the patterns perfectly overlap, indicating that the aging effect is not caused by the growth of primary particles. Moreover, as rutile (the thermodynamically stable titania phase) was not formed by aging, this indicates that the dissolution–reprecipitation is very limited.

Actually the aging effect can be due to the fact that the densification of aggregates is a slow process with a time scale of several days. During the initial hydrolysis step, the very fast agglomeration process is diffusion-limited because there is no repulsion barrier and particles or clusters stick together each time they touch. Thus the aggregates are loosely packed and their fractal dimension is low ($1.5 < D_f < 1.7$). After the acid addition, adsorption of protons on the particle surface creates a repulsion barrier and the sticking probability decreases. A progressive reorganization of the aggregates toward a more compact packing is expected. To summarize, the effective volume fraction of the clusters is maximum after the sol synthesis and it decreases progressively as the fractal dimension of the aggregates increases. As pointed out by Vorkapic and Matsoukas [6], it is possible that when a packing density limit is reached, the aggregates cannot be peptized anymore.

Finally, we have assumed that PEG addition leads to the formation of more compact aggregates which explains why the aging effect on viscosity is very limited.

4. Conclusion

Titania hydrosols were prepared by fast hydrolysis of titanium alkoxide in a large excess of water. XRD patterns show that these sols contain nanocrystals (5–6 nm) of anatase (70%) and brookite (30%). TEM images indicate that these primary particles have a strong tendency to form aggregates whose mean hydrodynamic diameter, determined by photon correlation spectroscopy, is in the range of 80–90 nm

The flow curves of these colloids, recorded for several volume fractions of nanoparticles, can be perfectly fitted, in the range 0–100 s^{-1}, with a power-law model. In this range the behavior is Newtonian but for larger shear rates a shear thinning is observed.

The viscosity dependence on particle concentration can be predicted by a Batchelor-type model were the volume fraction of particles is replaced by an effective volume fraction of aggregates taking into account their fractal dimension.

Addition of PEG 2000 induced a marked decrease (about 50–60% of the value observed without PEG) of the sol viscosity down to a minimum. This decrease can be interpreted by assuming that PEG adsorbs on the surface of TiO_2 particles producing stabilization by steric effects and leading to formation of more compact aggregates.

The sol viscosity decreases on aging and this effect is strongly reduced after addition of PEG 2000. This transformation is not caused by the growth of primary particles. It is rather interpreted as a progressive reorganization of the aggregates toward a more compact packing.

References

[1] B. O'Regan, B.M. Gratzel, Nature 353 (1991) 737–740.
[2] O. Carp, C.L. Huisman, A. Reller, Prog. Solid State Chem. 32 (2004) 33–177.
[3] M. Haruta, Catal. Today 36 (1997) 153–166.
[4] T. Giornelli, A. Lofberg, E. Elisabeth Bordes-Richard, Appl. Catal. A 305 (2006) 197–203.
[5] G. Oskam, A. Nellore, R.L. Penn, P.C. Searson, J. Phys. Chem. B 107 (2003) 1734–1738.
[6] D. Vorkapic, T. Matsoukas, J. Colloid Interface Sci. 214 (1999) 283–291.
[7] B.L. Bischoff, M.A. Anderson, Chem. Mater. 7 (1995) 1772–1778.

[8] J.R. Bartlett, J.L. Woolfrey, in: L.L. Hench, J.K. West (Eds.), Chemical Processing of Advanced Materials, Wiley, 1992, pp. 23, 247–256.
[9] D. Vorkapic, T. Matsoukas, J. Am. Ceram. Soc. 81 (1998) 2815–2820.
[10] J.R. Bartlett, J.L. Woolfrey, Mater. Res. Soc. Symp. Proc. 271 (1992) 309–315.
[11] S. Music, M. Gotic, M. Ivanda, S. Popovic, A. Turkovic, R. Trojko, A. Sekulic, K. Furic, Mater. Sci. Eng. B 47 (1997) 33–40.
[12] G.J.A.A. Soler-Illia, C. Sanchez, New J. Chem. 24 (2000) 493–499.
[13] L. Zhang, Y. Zhu, Y. He, W. Li, H. Sun, Appl. Catal. B 40 (2003) 287–292.
[14] F. Bosc, A. Ayral, P-A Albouy, C. Guizard, Chem. Mater. 15 (2003) 2463–2468.
[15] S. Bu, Z. Jin, X. Liu, L. Yang, Z. Cheng, Mater. Chem. Phys. 88 (2004) 273–279.
[16] T. Miki, K. Nishizawa, K. Suzuki, K. Kato, Mater. Lett. 58 (2004) 2751–2753.
[17] T. Miki, K. Nishizawa, K. Suzuki, K. Kato, J. Mater. Sci. 39 (2004) 699–701.
[18] F. Bosc, A. Ayral, N. Keller, V. Keller, Appl. Catal. B 69 (2007) 133–137.
[19] J. Rodríguez-Carvajal, Commission Powder Diffraction (IUCr) Newslett. 26 (2001) 12–19.
[20] A.L. Patterson, Phys. Rev. 56 (1939) 978–982.
[21] S. Brunauer, P. Hemmett, E. Teller, J. Am. Chem. Soc. 60 (1938) 309–319.
[22] H. Zhang, J. Banfield, J. Phys. Chem. B 104 (2000) 3481–3487.
[23] J.W. Goodwin, R.W. Hughes, in: Rheology for Chemists: An Introduction, The Royal Society of Chemistry, London, 2002.
[24] A. Einstein, Ann. Phys. 19 (1906) 289–306.
[25] G.K. Batchelor, J. Fluid Mech. 83 (1977) 97–117.
[26] W.J. Tseng, K.-C. Lin, Mater. Sci. Eng. A355 (2003) 186–192.
[27] R. Prasher, D. Song, J. Wang, P. Phelan, Appl. Catal. Lett. 89 (2006) 133108.
[28] H. Chen, Y. Ding, Ch. Tan, New J. Phys. 9 (2007) 367.
[29] Y. He, Y. Jin, H. Chen, Y. Ding, D. Cang, H. Lu, Int. J. Heat Mass Transfer 50 (2007) 2272–2281.
[30] J. Chevalier, O. Tillement, F. Ayela, Appl. Catal. Lett. 91 (2007) 233103.
[31] S.M.S. Murshed, K.C. Leong, C. Yang, Int. J. Therm. Sci. 47 (2008) 560–568.
[32] T.D. Waite, J.K. Cleaver, J.K. Beattie, J. Colloid Interface Sci. 241 (2001) 333–339.
[33] R.J. Hunter, Foundations of Colloid Science, second ed., Oxford University Press, 2001.
[34] T.F. Tadros, Polym. J. 23 (1991) 683–696.
[35] J. Dutta, H. Hofmann, in: H.S. Nalwa (Ed.), Encyclopedia of Nanoscience and Nanotechnology, vol. X, pp. 1–23, www.aspbs.com/enn.